Investigation of the corrosion behaviour of TiC/Ti6Al4V manufactured through laser additive manufacturing.

Hosia Kgomo[1,2], *Bathusile* Masina[1,3], *Paul* Lekoadi[1,4], *Ipfi* Mathoho[1,3], *Thabo* Pesha[1], *Thabiso* Sibisi[5] and *Vusimusi* Mulaudzi[1].

[1]Photonic Center, Manufacturing Cluster, CSIR, South Africa
[2]Department of Chemistry, University of Limpopo, South Africa
[3]Department of Mechanical and Industrial Engineering Technology, University of Johannesburg, South Africa.
[4]Department of Material Science and Metallurgical Engineering, University of Pretoria, South Africa
[5]Department of Chemical, Metallurgical and Materials Engineering, Tshwane University of Technology, South Africa

Abstract. This research study focuses on investigating of the corrosion response of TiC/Ti6Al4V composite manufactured by laser additive manufacturing. Corrosion tests for TiC/Ti6Al4V were carried out with 3.5% of NaCl solution at room temperature 25ºC (remaining constant) and varying the time. Corrosion test results were used to obtain the Tafel plot graph, which determined the corrosion potential and current density of TiC/Ti6Al4V. Scanning electron microscopy (SEM) was used to analyse the microstructure of the material and X-ray diffraction (XRD) was used for phase analysis of the material. Comparison studies were done on the corrosion behaviour of TiC/Ti6Al4V and Ti6Al4V. TiC/Ti6Al4V showed better corrosion resistance than Ti6Al4V.

1 Introduction

Titanium alloys, such as Ti6Al4V (Ti64), have gained significant attention in various industries due to their exceptional combination of high strength-to-weight ratio, corrosion resistance, and biocompatibility [1-2]. However, at high temperatures, Ti64 is susceptible to oxidation and corrosion, leading to the degradation of its mechanical properties and limiting its use in demanding applications [3].

Hee et al. (2016) coated Ti64 with Ta in order to improve the corrosion resistance of Ti64. In the study it was reported that the corrosion current of coated Ti64 was 2.4 x10^{-9} A·cm^{-2} at a slow scan rate while coated Ti64 showed similar low current density of 2.85 x10^{-9} A·cm^{-2}. It was concluded that Ta coating is a promising option to improve the corrosion resistance of Ti64 and further studies need to be done to confirm how do Ta coating improves the corrosion resistance of Ti64. From the study of Hee et al. (2016) it can be confirmed that there is no clear view of how Ta coating improves the corrosion resistance of Ti64, therefore Asgar et al. (2019) used graphene oxide to coat Ti64 in order to improve its corrosion resistance. From the results obtained, coated Ti64 showed improvement in electrochemical properties with a

low corrosion rate while uncoated Ti64 had a higher corrosion rate and mentioned that further investigation is still required. Jin et al. (2020) used alternative way (heat treatment) of improving the corrosion resistance of the Ti64. It was found that hot isotactic pressing attributed to the microstructure of Ti64, where the formation of more beta phase and less alpha prime was observed. The formation of the beta phase resulted in an increase in the corrosion resistance of Ti64. From above mentioned studies/many researchers focus on improving the corrosion of the material by post-processing and surface coating which require more time [4]. An alternative way of improving the corrosion resistance of Ti64 is to add ceramics such as TiC or TiB_2 due to their high hardness and strength. The addition of ceramic TiC or TiB_2 to Ti64 forms a titanium-based matrix composite. Pan et al. (2022) used a titanium-based matrix composite to improve the mechanical properties (strength and ductility) of Ti64. It was reported that titanium-based matrix composite had unique network microstructure which had an exceptional impact on mechanical properties. Ti64-based matrix composites are promising materials as they have shown great potential in improving the mechanical properties of Ti64, therefore in this study the corrosion behaviour of Ti64-based matrix composites manufactured through laser additive manufactured DED will be investigated.

Liu et al. (2023) investigated electrochemical corrosion of titanium-based matrix composite. It was found out that the addition of TiC refines the beta grains in the microstructure which resulted in improvement of corrosion resistance of Ti64 and said that "research on corrosion resistance of Ti64-based matrix composites fabricated by DED is still lacking". Understanding the corrosion behaviour of Ti64-based matrix composites manufactured via additive manufacturing (AM) is critical to their safe and effective use in various applications.

The response to corrosion of Ti64-based matrix composites produced through AM is essential to determine their suitability for specific applications and to develop strategies to mitigate any potential corrosion-related issues as it is envisaged that the product will have a significant improvement as compared to the conventional process of Ti64-based matrix manufacturing. Ti64-based matrix composites are promising materiald for high-temperature applications due to their high strength and good corrosion resistance [9]. This research can lead to the development of improved corrosion-resistant Ti64-based matrix composites, ultimately improving the performance, durability, and safety of the end products.

2 Methodology and results

Fig. 1 shows the DED system and components. The TiC/Ti64 and Ti64 were fabricated using a laser additive manufacturing technique (DED). One of the major components of the DED system is the KUKA robotic arm for easy movement, the powder feeder system for delivering the powders (Ti64 and TiC) into the melt pool created by a focused energy source of the 1073 nm, IPG fiber laser, which enables the layer-by-layer fabrication of the TiC/Ti64 composite and Ti64 samples. The laser energy density used to manufacture all the samples was 90 J/mm. Argon gas was used as the carrier, 1.5 l/min and shielding gas, 15 L/min. Since TiC/Ti64 is fabricated by in-situ process, the mass percentage of TI64 was 95% while for TiC was 5% and for as-built Ti64 the mass percentage was 100%.

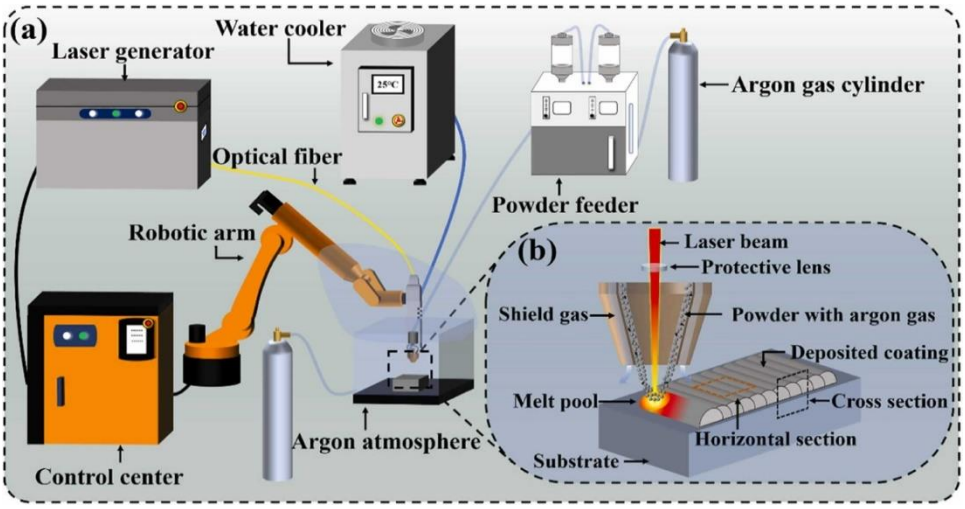

Fig. 1. Direct Energy Deposition system [9].

2.1 Sample preparation and material characterization

The samples were cut into square shapes (1x1 cm) using cutting machine and mounted on resin and polished to a mirror-like finish. The microstructure of the sample was analysed using scanning electron microscopy (SEM) and X-ray diffraction (XRD) was used for phase analysis of the material to obtain initial the microstructure and phase analysis of TiC/Ti64 and Ti64 before running the corrosion test.

2.2 Electrochemical experiment

Fig. 2 shows the electrochemical system (potentiostat) used to conduct the corrosion test. 3.5% of NaCl was prepared in 500ml of distilled water with a mass of 17.62 g. Silver-Silver chloride (SSC or Ag/AgCl) was used as the reference electrode and the Pt sheet was used as the auxiliary electrode. The corrosion test of TiC/Ti64 and Ti64 was carried out with 3.5% of NaCl solution at room temperature 25º (remaining constant) with varying time and electrochemical tests such as open circuit potential (OCP) and potentiodynamic polarization were done. The microstructures of the samples were analysed again using SEM after corrosion testing.

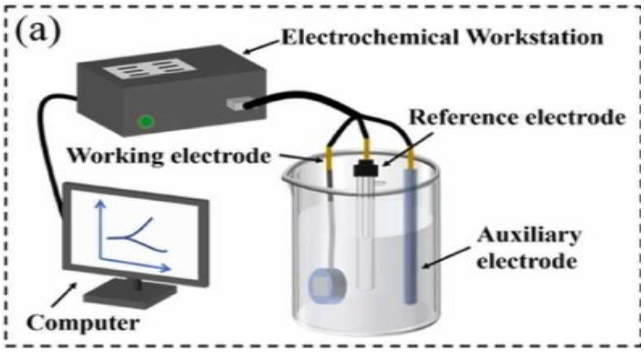

Fig. 2. Electrochemical system setup [10]

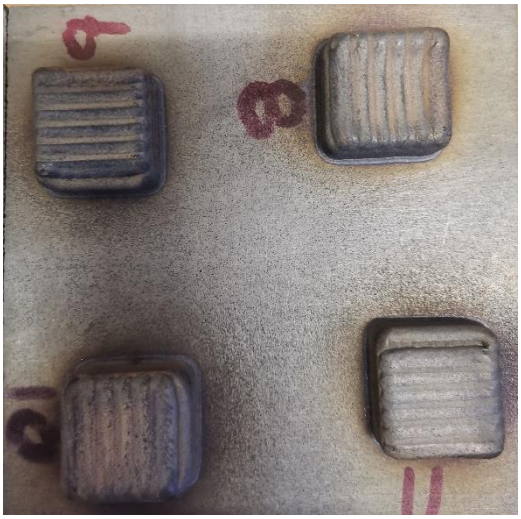

Fig. 3. As-built cube samples of TiC/Ti64

2.3 Microstructure analysis

Fig. 4 (a) below shows an overview of the SEM microstructure of as-built TiC/Ti64 fabricated with laser additive manufacturing using the DED technique. The microstructure present in TiC/Ti64 is not homogeneous across the sample. It is observed that there is an existence of a novel/network microstructure in certain parts of the microstructure whereas a certain portion of the microstructure consists of randomly arranged TiC dendrites [10]. The microstructure also shows the presence of unmelted TiC and porosity. The cause of the microstructure not being homogeneous across the sample may be caused by several factors such as thermal gradient, composition segregation and process parameters [10]. Fig. 4 (b) shows the alpha and beta phases in the microstructure, due to the presence of Ti64 which is an alpha-beta alloy [12]. The existence of the alpha phase and beta phase in TiC/Ti64 was verified by the study conducted by Bai *et al.* (2019) which reported that the cellular morphology of the TiC phase is enclosed in TiC/Ti64 which contains a mixture of alpha and beta grains showing equiaxed microstructure with alpha grains being grey occurring inside the beta matrix and beta phase being lighter than the alpha phase . Fig. 4 (c) shows the microstructure of TiC/Ti64. From the image the novel/network microstructure can be observed which contains TiC at grain boundaries. The presence of TiC at grain boundaries was confirmed by the study conducted by Bai *et al.* (2019) using the Electron backscatter diffraction (EBSD) technique [13]. The presence of the TiC phase is also validated by XRD in Fig. 4. Fig. 4(d) shows TiC/Ti64 at high resolution with TiC/Ti64 at grain boundaries.

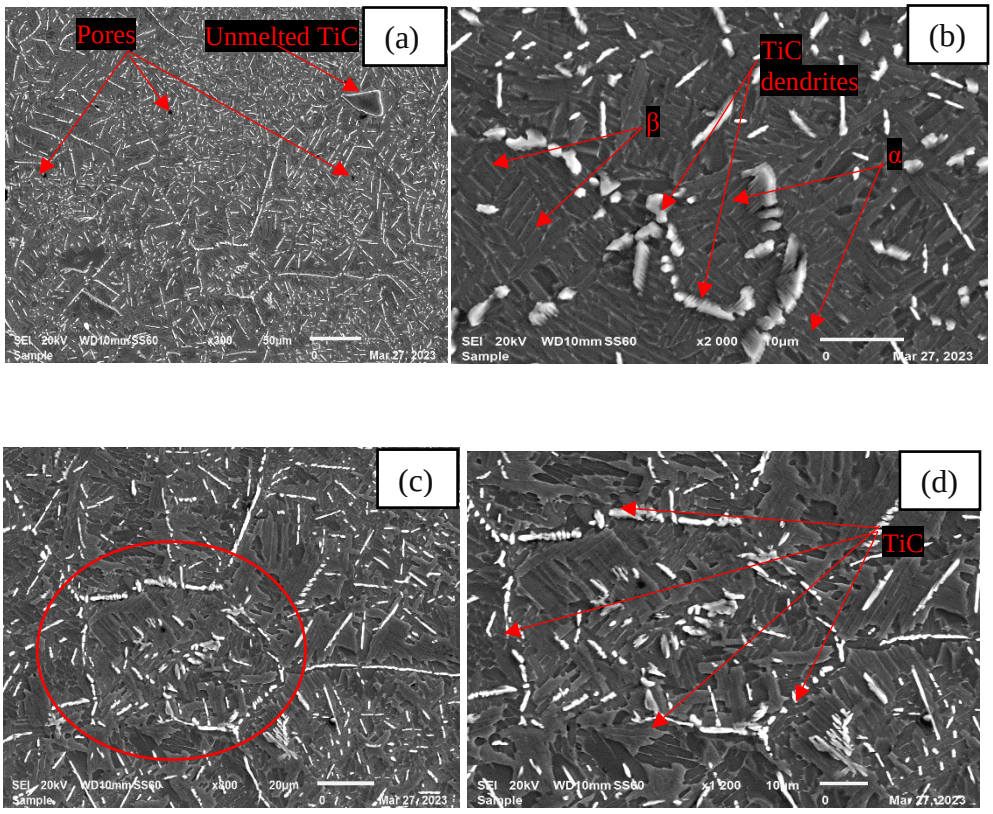

Fig. 4. SEM microstructure of as-built TiC/Ti64 (a) x300 magnification, (b) x200 magnification and (c) x800 magnification and (d) x1200 magnification.

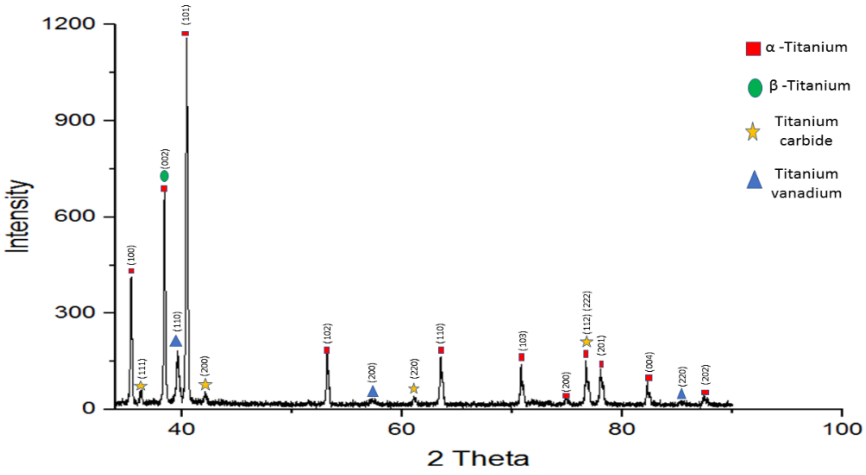

Fig. 5. XRD spectrum of as-built TiC/Ti64.

Fig. 6(a) presents the SEM microstructure of the as-built Ti64 at x300 magnification manufactured through the DED process. The microstructure differs according to techniques used, and process parameters and, in this case the as-built Ti64 shows a lamellar microstructure [14]. It is observed that there is a long grain boundary, which is normally caused by uneven growth when the material is crystallizing. The grain boundary is one of the preferred sites of corrosion including pores. Fig. 6(b) shows high magnification of the grain boundary. Fig. 6(c) shows the presence of lamellar β with white colour and lamellar α inside [16].

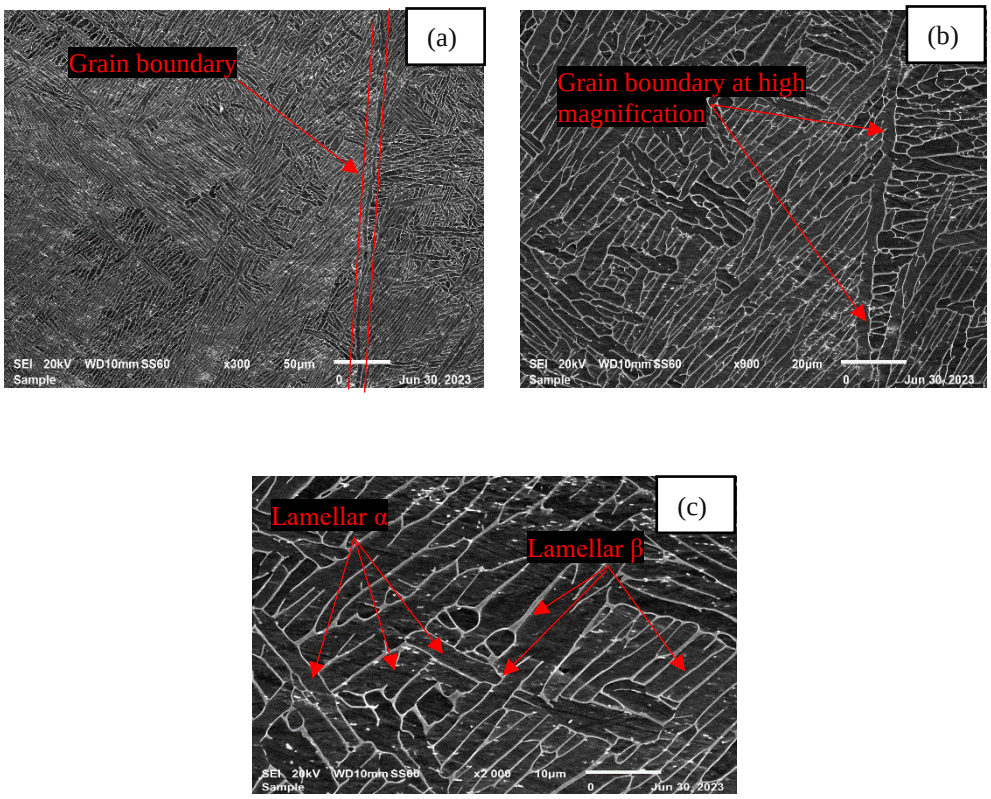

Fig. 6. SEM microstructure of as-built Ti64 (a) x300 magnification, (b) x900 magnification and (c) x2000 magnification.

Fig. 7(a) shows the SEM microstructure of as-built TiC/Ti64 which was discussed in Fig. 4 (a). Fig. 7(b) and Fig. 7(c) show the surface of TiC/Ti64 at 2 hours and 4 hours respectively after corrosion testing. In both TiC/Ti64 at 2 hours and 4 hours there is a presence of porosity that was caused by corrosion. Corrosion typically occurs at locations where pores exist within the material structure, leading to the enlargement of these pores, which, in turn, adversely impacts the material's properties. In light of the provided images, the presence of white-coloured sodium chloride (NaCl) inside these pores is indicative of corrosion activity targeted at these porous areas. [14]. The presence of NaCl inside the pores was confirmed by EDS in Fig. 9.

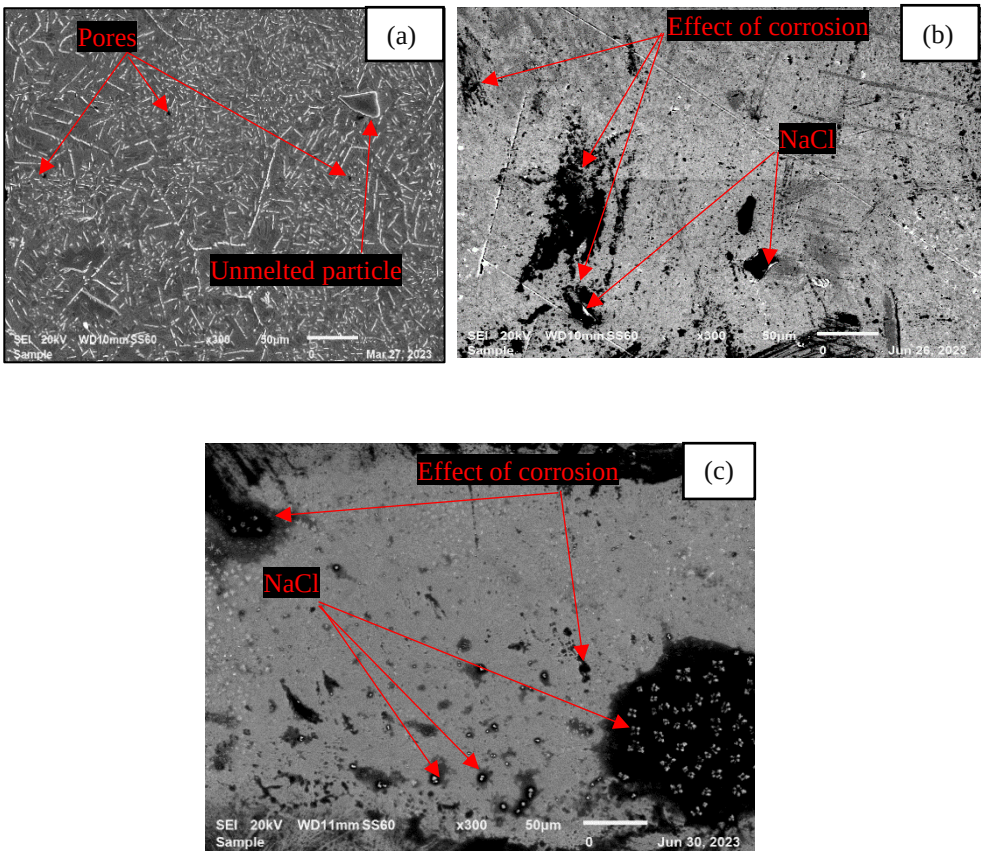

Fig. 7. SEM images (a) as-built TiC/Ti64, (b) Corrosion tested TiC/Ti64 at 2 hours and (c) Corrosion tested TiC/Ti64 at 4 hours all at x300 magnification.

Fig. 8 (a) presents the SEM microstructure of the as-built Ti64 which was discussed in Fig. 5(b). Fig. 8 (b) and (c) present the surface of Ti64 at 2 hours and 4 hours respectively after being subjected to corrosive environment of 3.5% of NaCl. There is an appearance of pores in Ti64 at 2 hours and 4 hours which were induced by corrosion reaction. NaCl is present inside pores caused by corrosion [16]. The presence of NaCl inside the pores was confirmed by EDS in Fig. 9.

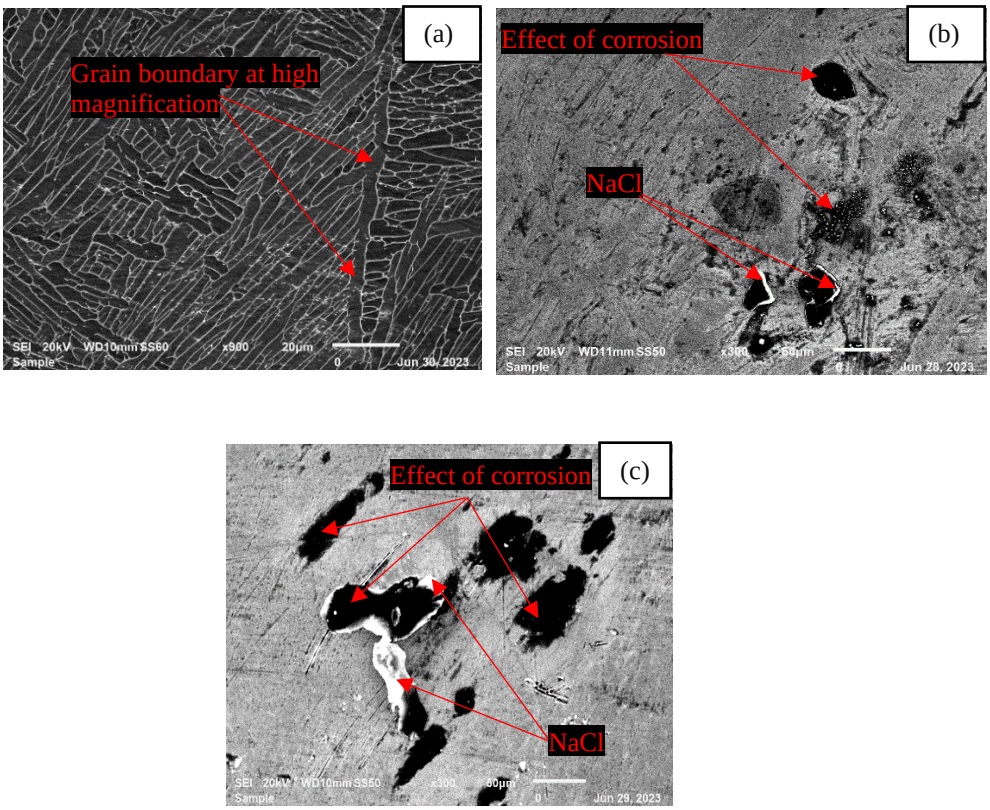

Fig. 8. SEM images (a) as-built Ti64, (b) Corrosion tested Ti64 at 2 hours and (c) Corrosion tested Ti64 at 4 hours all at x300 magnification

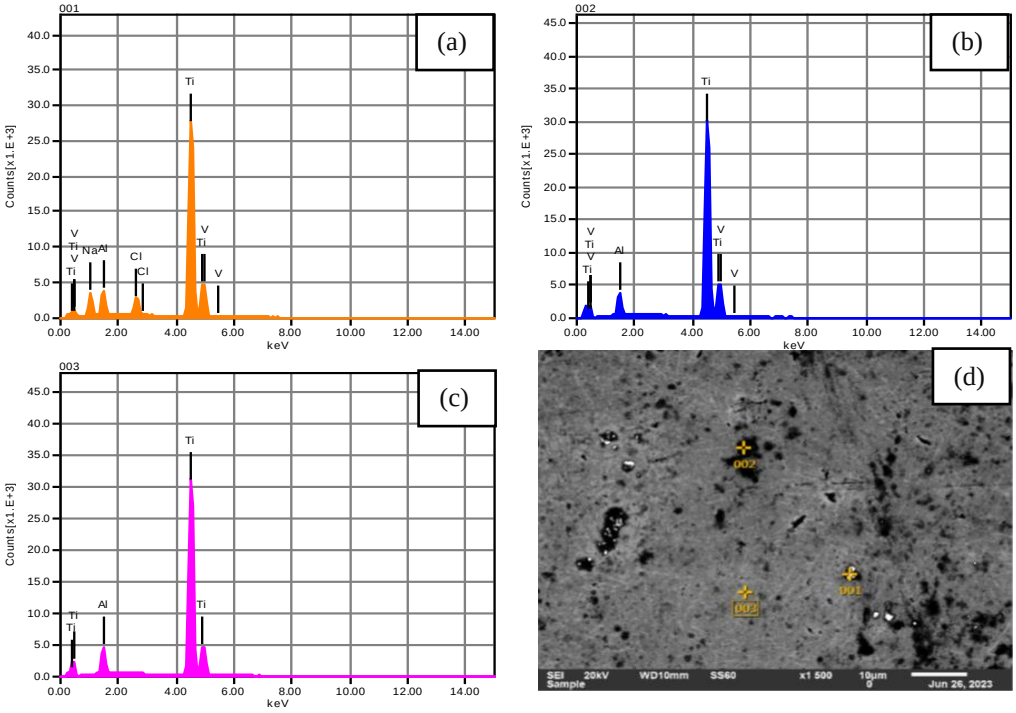

Fig. 9. (a), (b) and (c) shows the elements present in the sample and (d) shows the EDS analysed points

2.4 Electrochemical analysis

Fig. 10 shows the open circuit potential (OCP) of Ti64 and TiC/Ti64 which were exposed to a corrosive environment (3.5% of NaCl) for 2 hours at room temperature. In general, OCP gives an indication of the behaviour of the material in a corrosive medium and it is known that the material with higher corrosion resistance is characterized by higher values of corrosion potential [17]. From the OCP of TiC/Ti64 it was observed that initially the graph was constant and around the 1900s the graph slightly increased and this can be caused by the presence of pores in the sample [observed in Fig. 7 (a)]. Overall, it was observed that TiC/Ti64 is linear from the start to the point, and this is due to the presence of TiC at grain boundaries protecting the inner phases of the material against further corrosion. TiC/Ti64 showed no formation of a clear passive layer (confirmed in Fig. 12) but, in OCP graph confirms that TiC/Ti64 experienced a short-term corrosion reaction, and this is due to the presence of TiC in the material. The formation of the passive layers in Ti64 took longer to form than in TiC/Ti64 due to the lack of protection in the inner phases of Ti64, because of the prior beta grains presence.

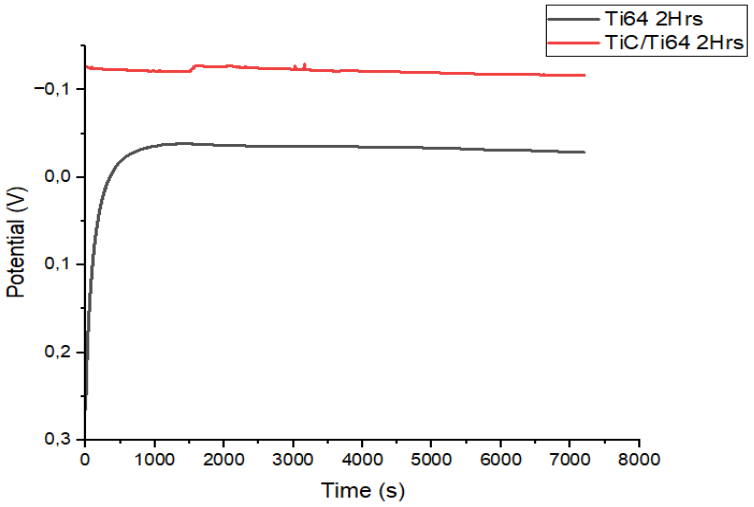

Fig. 10. OCP graph of Ti64 and TiC/Ti64 at 2 hours.

Fig. 10 shows the OCP of Ti64 and TiC/Ti64 under the same conditions mentioned in the above discussion but, with different exposure times which in this case was 4 hours. In this experiment the behaviour of TiC/Ti64 is different from the one observed in Fig. 10. In this OCP graph TiC/Ti64 still showed no clear formation of a passive layer (confirmed in Fig 12), but it shows that TiC/Ti64 started to stabilize around -0.09 V which indicates that the material has reached a state of electrochemical equilibrium, where the corrosion rate remains relatively constant over time and it indicates that the material is relatively resistant to further corrosion in the given environment. The stabilization of the TiC/Ti64 layer started around 1500 s whereas in Ti64 the formation of the passive layer started around 3600 s. Although there is a slight difference in the stabilization of these two materials at a specific time, the stabilization of Ti64 occurs at more of a negative potential which indicates that it is more prone to corrosion. It can be confirmed from these OCP's that TiC/Ti64 and Ti64 stabilized at different times due to microstructure differences such as the presence of TiC at the grain boundaries of TiC/Ti64 [8].

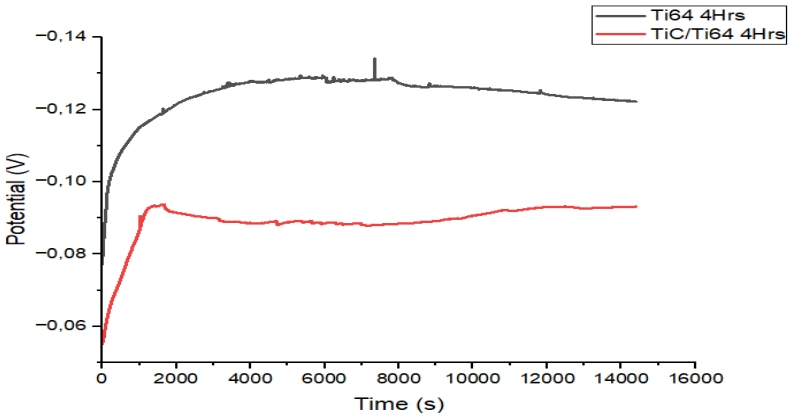

Fig. 11. OCP graph of Ti64 and TiC/Ti64 at 4 hours.

Fig 12 presents the Tafel plots of all tested material Ti64 and TiC/Ti64 immersed in corrosive environment(3.5% of NaCl solution) and all these polarization curves start around the same point with a slight absence of cathodic region which indicates that the formation of the passive layer occurs very fast and also TiC protection, which can also be confirmed OCP's presented in Fig 10 and 11. The polarization curves of Ti64 for 2 and 4 hours have a shorter cathodic region than TiC/Ti64 and this is due to the passive layer and TiC protection. The formation of a layer in Ti64 is clear due to its polarization curves becoming more linear after the anodic region and in TiC/Ti64 there is no clear formation of a passive layer as its polarization curves continue to the positive side of current and potential. As explained in Fig. 10 that due to the presence of TiC which enhances the formation of a solid protective layer in TiC/Ti64, hence TiC/Ti64 takes longer to reach the anodic region than Ti64 [8].

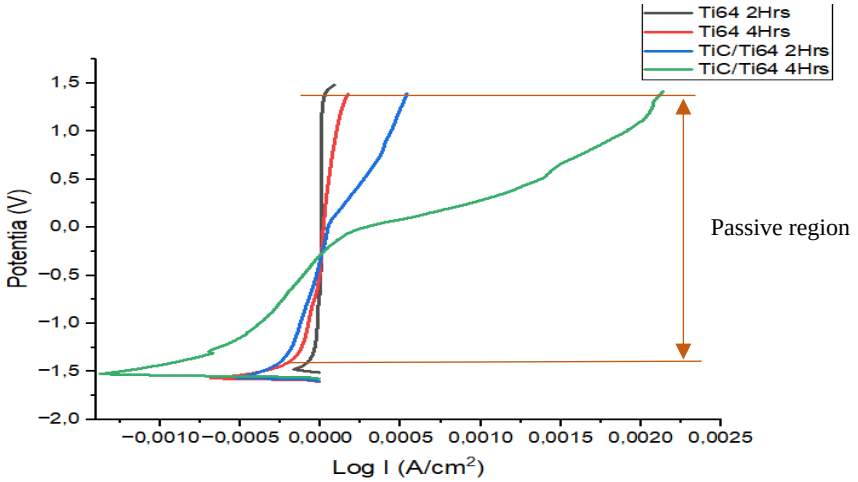

Fig. 12. Tafel data of Ti64 2 hours, TiC/Ti64 2 hours, Ti64 4 hours and TiC/Ti64 4 hours.

Fig. 13 presents the classic Tafel analysis where the corrosion current (Icorr) and corrosion potential (Ecorr) in an electrochemical cell are estimated using the mathematical technique known as tafel extrapolation. The linear sections of the anodic and cathodic plots are extended back to their intersection to perform extrapolation. The corrosion current Ecorr and Icorr are obtained at the point where these two lines intersect. The eequations used to extrapolate/calculate Ecorr, Icorr and Jcorr are listed from equation (1) to (6) [18].

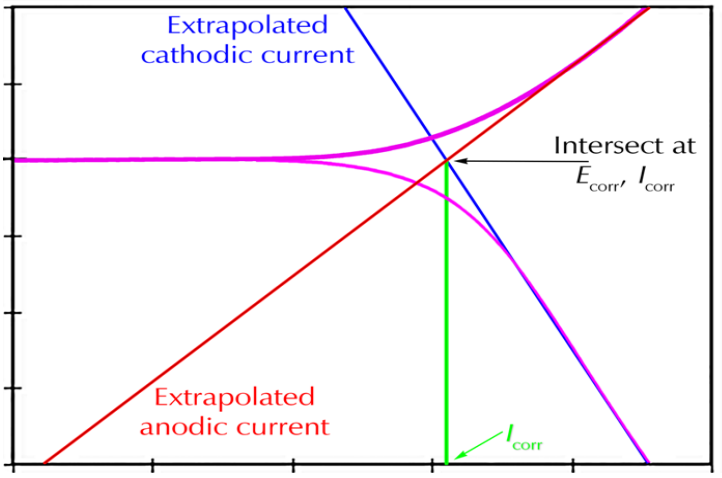

Fig. 13. shows classic Tafel analysis [19]

General equation of a tangent

$Y_1 = mx + c$, for both anodic tangent (1)

$Y_2 = mx + c$, for cathodic tangent, where : (2)

$Y_1 = Y_2$, therefore: (3)

$y = E_{corr}$ (Corrosion potential at the intersection of anodic tangent and cathodic tangent) (4)

$x = I_{corr}$ (Corrosion current Corrosion potential at the intersection of anodic tangent and cathodic tangent) (5)

Current density (J_{corr})

$J_{corr} = I_{corr}/A$ (A/cm^2) (6)

Table 1 presents the electrochemical corrosion parameters of Ti64 at 2 hours, TiC/Ti64 at 2 hours, Ti64 at 4 hours and TiC/Ti64 at 4 hours. From the fundamentals of corrosion kinetics, it is stated that the current density is directly proportional to the corrosion. From the table below TiC/Ti64 had a less negative current density of -3,61 $X10^{-05}$ A/cm^2 which indicates that TiC/Ti64 at 2 hours performed well or had higher corrosion resistance than all other samples, this can also be confirmed by the OCP in Fig. 10 where the graph was linear form the start to the end showing no corrosion reaction [17]. It is very rare for current density and corrosion rate to be negative but, it is possible due to the formation of the passive layers which act as a barrier against further corrosion. The negative current density and corrosion rate show that there is a gain of mass on the sample, and this is due to the formation of the passive layers. In a normal corrosion test it is expected to see material corroding but, in this case, the material is different due to the presence of TiC. For 4 hours samples TiC/Ti64 had a less negative current density of -9,65 $X10^{-05}$ which indicates that it has high corrosion resistance [9].

Table 1. Electrochemical corrosion parameters of Ti64 2 hours, TiC/Ti64 2 hours, Ti64 4 hours and TiC/Ti64 4 hours.

Materials	E_{corr} (V)	J_{corr} (A/cm^2)	I_{corr} (A)
TiC/Ti64 2 hours	-0,33042	-3,61 X10^{-05}	-3,61 X10^{-05}
Ti64 2 hours	*-0,5837*	-1,78 X10^{-06}	-1,78 X10^{-06}
TiC/Ti64 4 hours	-0,28525	-9,65 X10^{-05}	-9,65 X10^{-05}
Ti64 4 hours	-0,37548	-9,01 X10^{-06}	-9,01 X10^{-06}

3 Conclusion

The corrosion behaviour of TiC/Ti64 and Ti64 was successfully investigated. Overall, TiC/Ti64 exhibited a linear OCP behaviour, reflecting the protective role of TiC at grain boundaries, preventing further corrosion. While it showed no formation of a clear passive layer, the OCP graph showed minimal corrosion due to TiC presence. Furthermore, in the OCP graph analysis of 4-hour exposure time, TiC/Ti6Al4V exhibited a similar absence of a clear passive layer, but the graph stabilized around -0.09 V, where Ti64 took longer to form a passive layer, starting at around -0.13 V at a more negative potential. Additionally, the Tafel plots provided insight into the rapid formation of passive layers in Ti64. TiC/Ti64 and Ti64 exhibited shorter cathodic regions due to the presence of a passive layer in Ti64 and TiC in TiC/Ti64. In contrast, TiC/Ti64's polarization curves extended to the positive side of current and potential, as the absence of a clear passive layer allowed the material to resist anodic reactions. TiC/Ti64 showed superior corrosion resistance due to the ceramic (TiC) present and its unique microstructure. The addition of TiC to Ti64 can now be confirmed that it increases the corrosion resistance of Ti64.

I would like to acknowledge Tshwane University Technology physical metallurgy laboratory with assistance from Mr Thabiso Hopewell and also acknowledge my colleagues from Laser Enable Manufacturing with assistance in the laboratory and the University of Limpopo Department of Chemistry. This research was funded by the Department of Science and Innovation (DSI) of South Africa (SA) through the Collaborative Program in Additive Manufacturing (CPAM), grant number HLM4BMX.

Reference

1. P. Herrera, E. Hernandez-Nava, R. Thornton and T. Slatter . Abrasive wear resistance of Ti-6AL-4V obtained by the conventional manufacturing process and by electron beam melting (EBM), (2023).

2. E.T. Akinlabi, I. Mathoho, M.P. Mubiayi, C. Mbohwa and M.E. Makhatha, "Effect of process parameters on surface roughness during dry and flood milling of Ti-6A-l4V," 2018 IEEE 9th International Conference on Mechanical and Intelligent Manufacturing Technologies (ICMIMT), Cape Town, South Africa, pp. 144-147, (2018).

3. J. Dai, J. Zhu, C Chen and Weng, F. High temperature oxidation behavior and research status of modifications on improving high temperature oxidation resistance of titanium alloys and titanium aluminides: A review. Journal of Alloys and Compounds, (2016).

4. Qian, H. Xu and Q. Zhong. The influence of process parameters on corrosion behaviour of Ti6Al4V alloy processed by selective laser melting. Journal of Laser Applications, (2020).

5. L. Hee, A.C. Jamali, S.S Bendavid, A Martin, P.J. Kong and Y. Zhao. Corrosion behaviour and adhesion properties of sputtered tantalum coating on Ti6Al4V substrate. Surface and Coatings Technology, 307, pp.666-67, (2016).

6. H. Asgar, K.M. Deen, Z.U. Rahman, U.H. Shah, M.A. Raza, and W. Haider. Functionalized graphene oxide coating on Ti6Al4V alloy for improved biocompatibility and corrosion resistance. Materials Science and Engineering, 94, pp.920-928, (2016).

7. N. Jin, Z. Yan, Y. Wang, H. Cheng, and H. Zhang. Effects of heat treatment on microstructure and mechanical properties of selective laser melted Ti-6Al-4V lattice materials. International Journal of Mechanical Sciences, 190, pp.106042, (2021)

8. D. Pan, S Li, L. Liu, X. Zhang, B. Li, B. Chen, M. Chu, X. Hou, Z Sun, J. Umeda and K. Kondoh, K. Enhanced strength and ductility of nano-TiBw-reinforced titanium matrix composites fabricated by electron beam powder bed fusion using Ti6Al4V–TiBw composite powder. Additive Manufacturing, 50, p.102519, (2022).

9. X. Liu, S. Chen, J. Zhang, G. Yang, Y., Zhang, T. Wang and J. Lei. Enhancement of the electrochemical corrosion resistance of Ti6Al4V alloy reinforced by nano-and micro-TiC particles through directed energy deposition. Corrosion Science, pp.111343, (2023)

10. L.J. Huang, L. Geng, and H.X. Peng. In situ (TiBw+ TiCp)/Ti6Al4V composites with a network reinforcement distribution. *Materials Science and Engineering, (2010).*

11. H. Chen, D. Gu, D. Dai, C. Ma and M. Xia. Microstructure and composition homogeneity, tensile property, and underlying thermal physical mechanism of selective laser melting tool steel parts. *Materials Science and Engineering, (2017).*

12. S.A.S.M. Lampman. Wrought titanium and titanium alloys. *Properties and Selection: Nonferrous Alloys and Special-Purpose Materials*, (1990).

13. M. Bai, R. Namus, Y. Xu, D. Guan, M.W. Rainforth and B.J. Inkson. In-situ Ti-6Al-4V/TiC composites synthesized by reactive spark plasma sintering: Processing, microstructure, and dry sliding wear behaviour, (2019).

14. T. Niendorf, S. Leuders, A. Riemer, H.A. Richard, T. Tröster and D. Schwarze. Highly anisotropic steel processed by selective laser melting. *Metallurgical and materials transactions B, (2013).*

15. Y. Chong, T. Bhattacharjee and N. Tsuji. Bi-lamellar microstructure in Ti–6Al–4V: Microstructure evolution and mechanical properties. *Materials Science and Engineering, (2019).*

16. S.H. Ahn, J.H. Lee, J.G. Kim and J.G. Han. Localized corrosion mechanisms of the multilayered coatings related to growth defects. *Surface and Coatings, (2004).*

17. E.T. Akinlabi, I. Mathoho and M.P. Mubiayi, Corrosion behaviour and microhardness during dry and flood milling of Ti-6Al-4V alloy. Key Engineering Materials, 796, pp.91-96, (2019)

18. K. Park, B.Y. Chang and S. Hwang, Correlation between tafel analysis and electrochemical impedance spectroscopy by prediction of amperometric response from EIS. Acs Omega, 4(21), pp.19307-19313, (2019).

19. S. Frankel, Fundamentals of corrosion kinetics. Active protective coatings: new-generation coatings for metals, (2016).

RESPONSE TO COMMENTS

	Comments	Response
Reviewer 1	With which solution is a 3.5% NaCl concentration mixed?	Solution used was distilled water (added under methodology)
	Which type of LASER used for the fabrication of sample? And diameter of LASER?	The laser – IPG Fiber laser, 1073 nm (Added under methodology)
	What are the dimensional parameters of testing sample?	1x1 cm (added under methodology)
	A picture of 3D printed sample?	Picture of 3D printed samples was added.
	What criteria followed for selection for the printing parameters in DED and why?	Criteria selection – density of the sample (dense of the sample) and microstructure.
	Which equipment used for the corrosion test?	Potentiostat (added under methodology)
	What is the main purpose to perform OCP?	Stated under first discussion of OCP " In general, OCP gives an indication of the behaviour of the material in a corrosive medium "
	What are the equations used to find out the values of ECORR, JCORR AND ICORR	ECORR, JCORR AND ICORR were added
Reviewer 2	Stick to a single naming convention	The name was rectified to Ti6Al4V

	You mean DED?	Yes, LAM was removed from the statement and added DED (The introduction was changed by adding more of the literature)
	Do you have any information on the feedrate in grams/min? If not include a description of the powder feeder system	Description of the powder feeder system was added
	Define this for the audience (EBSD)	EBSD was defined (Electron Backscatter Diffraction)
	Fig. 4 is the XRD spectrum of the phases present	This caption was removed, since the caption of the spectrum was written below the figure.
	Please indicate this clearly in the microstructure or rephrase the sentence. Are you referring to grain boundary? I am not clear her	Yes, I was referring to the grain boundary
	I understand what you are trying to say but please rephrase. It is very confusing the way it is currently written.	The statement was rephrased to understandable statement.
	Why inverted commas?	Because of I was quoting the statement from above discussion, but inverted commas were removed
	Keep descriptions consistent NaCl?	Descriptions were kept consistent throughout the paper
	Please rephrase, avoid using informal Language	The statement was rephrased and formal language was used (Including comment A15)
	Is it figure 3a? Not 6?	Yes, the statement was corrected

	Not clear what you trying to say here an increase or more pronounced corrosion taking place in the composite?	The statement was rephrased to an understandable statement.
	Which figure?	Figure 10
	Add a bit more details in here. Summarise what you did	More details were added and summary of the experiment was added